



Original research article

Development of the house secreting epithelium, a major innovation of tunicate larvaceans, involves multiple homeodomain transcription factors

Yana Mikhaleva^a, Ragnhild Skinnes^{a,1}, Sara Sumic^a, Eric M. Thompson^{a,b}, Daniel Chourrout^{a,c,*}^a Sars International Centre for Marine Molecular Biology, University of Bergen, Thormøhlensgt, 55, N-5008 Bergen, Norway^b Department of Biology, University of Bergen, Norway^c Key Laboratory of Marine Genetics and Breeding, Ocean University of China, Ministry of Education, Qingdao 266003, China

ARTICLE INFO

Keywords:

Evolution
Novelties
Tunicates
Oikopleura
Homeobox
Fox

ABSTRACT

The mechanisms driving innovations that distinguish large taxa are poorly known and essentially accessible via a candidate gene approach. A spectacular acquisition by tunicate larvaceans is the house, a complex extracellular filtration device. Its components are secreted by the oikoplastic epithelium which covers the animal trunk. Here we describe the development of this epithelium in larvae through the formation of specific cellular territories known to produce distinct sets of house proteins (Oikosins). It involves cell divisions and morphological differentiation but very limited cell migration. A diverse set of homeobox genes, most often duplicated in the genome, are transiently and site-specifically expressed in the trunk epithelium at early larval stages. Using RNA interference, we show that two *prop* duplicates are involved in the differentiation of a region on and around the dorsal midline, regulating morphology and the production of a specific oikosin. Our observations favor a scenario in which multiple homeobox genes and most likely other developmental transcription factors were recruited for this innovation. Their frequent duplications probably predated, but were not required for the emergence of the house.

1. Introduction

The diversity of living organisms has been shaped by numerous anatomical and physiological changes, whose molecular causes are tentatively identified in evo-devo studies (De Robertis, 2008; Duboule, 2010; Wallace, 2002). Evolutionary developmental biology (evo-devo) studies the evolution of the developmental processes that leads to morphological variability between species. For changes that appeared during recent evolution, a potent way to identify their key determinants is forward genetics, using advanced model systems and closely related taxa. Novelty addressed in these ways are most often minor and do not include the acquisition or profound modification of tissues or organs. Understanding the origin of major novelties, which distinguish distantly related species, is usually based on candidate gene approaches, implemented on a background of ignorance concerning the type and number of genetic changes that have occurred. Among the mechanisms known to underlie novelties, changes in cis-regulatory elements have attracted considerable attention during the last two decades (Carroll, 2008; Koshikawa et al., 2015; Wray, 2007). Novelty could thus often originate from altered expression patterns of virtually unchanged genes. Changes in the coding sequence of key develop-

mental genes may however also explain significant alterations of the body plan (Galant and Carroll, 2002; Lynch and Wagner, 2008). The importance of newly created lineage specific genes in developmental mechanisms is also afforded increasing attention (Andersson et al., 2015; Tautz and Domazet-Lošo, 2011). Gene duplication was proposed as a potent source of innovations via changes of either coding sequences or regulatory elements (Andersson et al., 2015; Dittmar and Liberles, 2010; Ohno, 1970). It indeed suddenly creates a genetic redundancy, which can allow one or both duplicates to evolve a new function. Fifty years after gene duplication was introduced as an essential trigger of evolutionary changes, its real impact on the emergence of novelties tends to be relativized. This is partly because multiple studies have shown that a single gene can be made polyvalent by the addition of new regulatory elements. For vertebrates and many plant lineages that underwent whole genome duplication and therefore acquired numerous gene duplicates, there is abundant documentation of modified functions related to gene duplication, either novelties or increased specialization (Huminiček and Wolfe, 2004; Ming et al., 2015; Moriyama et al., 2016).

Phylogenetic studies have shown that tunicates are the closest living relatives of vertebrates, although anatomically, cephalochordates re-

* Corresponding author at: Sars International Centre for Marine Molecular Biology, University of Bergen, Thormøhlensgt, 55, N-5008 Bergen, Norway.

E-mail address: daniel.chourrout@sars.uib.no (D. Chourrout).¹ Present address: Institute for Clinical Medicine, University of Oslo, Norway.

semble vertebrates more (Delsuc et al., 2006). Tunicates have evolved more rapidly and were probably simplified from more complex ancestors. While their phylogenetic position nearer the vertebrates results from the comparison of conserved gene sequences, their overall genome organization and gene complements are also divergent (Denoeud et al., 2010). A relatively large number of ancestral chordate genes, including key developmental genes, have been lost or were not detected in tunicate genome sequences (Denoeud et al., 2010; Wada et al., 2003). Among tunicates, the larvaceans that retain the chordate tail in the adult stage have evolved even more rapidly than the sessile ascidians. Approximately one quarter of the ancestral homeobox gene groups were not detected in the genome of *Oikopleura dioica* (Edvardsen et al., 2005), a larvacean that can be routinely cultivated and bred over a very short life cycle. Interestingly, a similar proportion of homeobox genes have been duplicated in the *O. dioica* genome, and most of these are transiently expressed in the epithelium of the larval trunk (Denoeud et al., 2010). This monolayer of cells gives rise to the highly specialized « oikoplastic epithelium » which after metamorphosis produces and secretes the components of the *O. dioica* « house » (Spada et al., 2001). A recent study of the epithelium patterning process, showed that the complex epithelial fields form in an invariant manner at the single cell level (Kishi et al., 2017). The house, a particularly spectacular innovation found in all larvaceans, serves to filtrate and concentrate food particles, mainly bacteria and microalgae. It contains multiple filters and chambers, and it is regularly replaced by a newly inflated pre-house rudiment. The distinct regions of the pre-house accurately match well differentiated and delimited cellular territories of the oikoplastic epithelium, named after zoologists, which possess a fixed number of cells with characteristic nuclear sizes and shapes (Ganot and Thompson, 2002). The pre-house mainly consists of an assembly of cellulose, that tunicates can synthesize (Sagane et al., 2010) with at least 80 highly glycosylated proteins named Oikosins (Hosp et al., 2012; Sagane et al., 2011; Spada et al., 2001). Genes that encode Oikosins are specifically expressed in given territories of the epithelium. These genes and the encoded proteins have no identifiable orthologs in metazoans other than larvaceans.

Here, we first describe oikoplastic epithelium development after observing the formation of distinct cellular territories. To elucidate the developmental mechanisms at work during this process, we initiated a candidate gene approach, beginning by mapping the expression of multiple homeobox genes on the epithelium. Most of these genes have been duplicated and we studied in more detail the expression patterns of two *prop* and three *otx* genes. The involvement of both *prop* genes in the fate of epithelial cells around the dorsal midline and one of their secreted Oikosin products is shown by RNA interference. This study supports a recruitment of multiple homeodomain transcription factors in pathways organizing one of the most elaborate innovations of chordate evolution.

2. Results

2.1. Development of the oikoplastic epithelium

To follow the development of cellular fields within the oikoplastic epithelium, larvae were collected and their nuclei stained with SYBR-green, every hour from hatching (4 hpf) to metamorphosis (11 hpf) (Fig. 1). Expression of seven Oikosin genes, which encode house proteins, was monitored by ISH during the same period (Fig. S1). In the tadpole just after hatching (4 hpf), the distribution of nuclei and their sizes were rather uniform, precluding the recognition of future territories from this early stage. However larger than average internuclear spaces were already observed in a dorsal and anterior location, which may correspond to the Giant Fol anlage (Fig. 1, 4hpf). Cells located immediately anterior to it indeed express *oikosin5* as early as 4 hpf, a gene that is later on specifically active in the Anterior Fol field. (Fig. 1). Another row of nuclei separated by large internuclear space is

situated posterior and may correspond to the Posterior Fol Field. Nuclei situated between the Anterior and Posterior Fol belong to the Nasse cells. Eisen cells were distinguishable at 5 hpf, though not yet at their final, more anterior position, that they reached in two more hours through collective migration.

At 6 hpf, most epithelial territories were discernible through their distinctive nuclear shapes and spacing (Fig. 1), with a strict bilateral symmetry around the dorsal midline. Anterior Fol cells were organized in two oval shaped groups. Giant Fol cells were aligned in one row on each side of the dorsal midline. Nasse nuclei were relatively smaller, and aligned in three consecutive rows on each side. At 7 hpf, the epithelium had differentiated into definitive nuclear fields, but not all cells were yet present. The total number of epithelial cells doubled between 4 and 5 hpf and doubled again between 5 and 7 hpf (Fig. S3.5). It continued to increase at a slower rate until 8 hpf, when epithelial morphology was very similar to that of the adult. Then, cell sizes began to increase, and as a consequence, the nuclei became gradually less tightly packed. Comparison of cellular positions between different developmental stages did not provide evidence supporting potential cell migration, with the already mentioned exception of the Giant Eisen field. This territory attained its final number of cells at 5 hpf, as did the Giant Fol two hours later, exactly when transcripts of the *oikosin1* gene first appear in this field (Fig. S1). Initial expression of *oikosin5* was detected in the Anterior Fol at 4 hpf, followed at 5 hpf by expression of *oikosin3* (Fig. S1), suggesting an early differentiation of cells in this field. These continued to divide until metamorphosis, but most divisions occurred between 4 and 6 hpf. In the other regions, the number of cells also increased faster at early as opposed to later larval stages and most oikosin genes commenced expression at 6–7 hpf (Fig. S1). Our observations in the increment of cell numbers and formation of the different epithelial fields are congruent with live imaging data of post hatching epithelium development obtained in the H.Nishida laboratory (Kishi et al., 2017).

3. Expression of transcription factors in the developing oikoplastic epithelium

In a partial ISH screen for the expression of homeobox transcription factor genes, we noticed that a significant proportion of them were expressed in the trunk epithelium of early larvae (Denoeud et al., 2010). Their expression patterns were highly regionalized and appeared earlier than those of Oikosin genes. They were therefore compatible with a role in patterning the oikoplastic epithelium (Fig. 2). Their transcripts were found in three main areas: anterior - in epithelial cells surrounding the mouth (*otxA*, *otxC*, *pax37A*, *irxC*, *dlx1*, *dlx2*), central - in domains more or less coinciding with the precursors of the Fol, Anterior rosette and Martini fields (*otxA*, *otxB*, *otxC*, *propA*, *propB*, *pax37A*, *pax37B*, *irxA*, *irxC*), and posterior - in domains leading to the Posterior rosette and other posterior dorsal cells (*irxA*, *irxC*, *dlx1*, *dlx2*, *emx*, *notB*). We also performed ISH for 11 Fox transcription factor genes and ISH revealed that at least seven were also expressed in the larval epithelium (Fig. S2.2). Interestingly, most homeobox genes found to be expressed in the early larval epithelium are duplicated (or tri- or quadruplicated) in the *Oikopleura* genome (Denoeud et al., 2010). In most situations, both duplicates were expressed in the epithelium, often within the same region.

To investigate the evolution of duplicated homeobox genes that may contribute to patterning of the oikoplastic epithelium, we focused on the two *prop* genes and the three *otx* genes of *O. dioica*. In the few species where *prop* genes have been studied, including vertebrates, there is a single *prop* gene. The *prop* gene of vertebrates plays an important role in the development of the pituitary gland (Angotzi et al., 2011; Nakamura et al., 1999; Sornson et al., 1996). In the ascidian tunicate *Ciona intestinalis*, the embryonic and larval expressions of *prop* are restricted to the sensory vesicle (Imai et al., 2004). Both the epithelial expression and the duplication of *prop* in *O. dioica* are

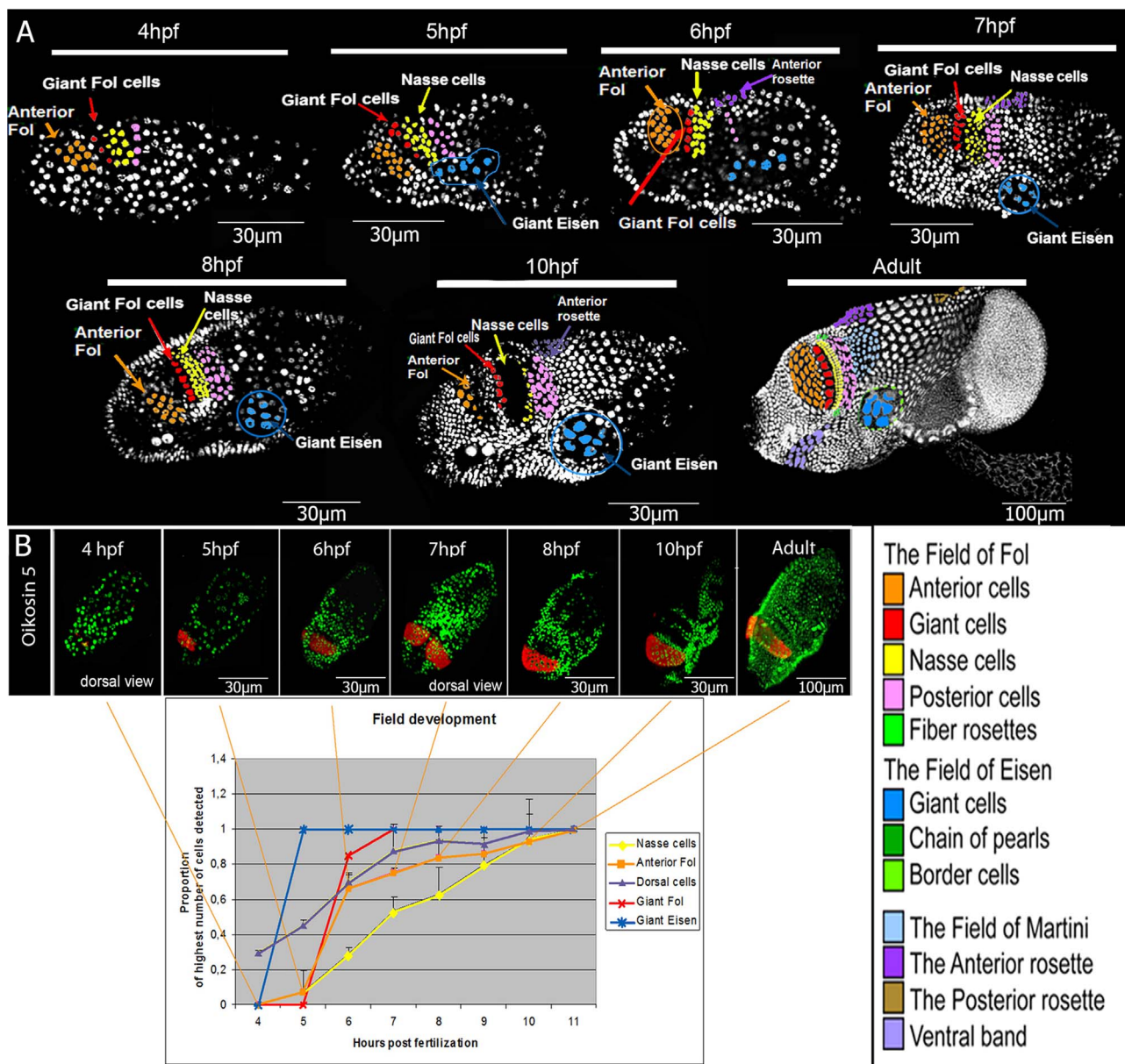


Fig. 1. Epithelial development from hatching to metamorphosis. Day 2 animals were used as reference for naming the distinct cell territories of the adult. All larvae oriented anterior to left. **A.** At 4 hpf the prospective Giant Fol cells (red), Anterior Fol cells (orange), Nasse cells (yellow) and Posterior Fol cells (pink) are marked. At 5 hpf Giant Fol cells were easily recognizable and almost all of them were in their final locations. Giant Eisen cells (blue) stopped dividing at this point and started to migrate to their final position. At 6 hpf all epithelial fields were easy recognizable and the Anterior rosette (purple) was evident. At 7 hpf Giant Eisen cells reached their final destination and Giant Fol cells attained their final number. From 8–10 hpf cells in some regions continued to divide and differentiate, and the epithelium came to resemble that of the adult. **B.** Proportional increases in cell numbers of five selected fields were followed. Developmental expression of the *oikosisin5* gene is shown to illustrate increasing cell numbers during formation of the Anterior Fol. Expression of *oikosisin5* was first observed immediately after hatching, in 2–4 anterior cells, and gradually increased in area in concert with the number of cells in the Anterior Fol. Other *oikosisin* gene expression patterns during development are shown in Supplementary Fig. S1.

consequently lineage-specific. In contrast to most duplicated genes of *O. dioica* (Denoeud et al., 2010), the *prop* gene duplicates colocalize in one genome site in opposite orientation, with no intervening genes. Both genes have three introns, of which one occurs in both genes at the conserved position encoding residues 44/45 of the homeodomain. Therefore, the duplication most likely occurred through a genomic rearrangement, and not through retroposition. The duplication could be relatively old since we systematically find orthologs of each *O. dioica* *prop* gene in new genomes sequences from other Oikopleurid species (see Fig. S3.2). Their tandem arrangement in opposite orientation is also observed in at least *O. albicans* and the more distantly-related *O. longicauda*. In *O. dioica*, *propA* began to be expressed before hatching in two posterior cells of the cerebral ganglion (Fig. S2.1, ABCD). The ISH signal vanished from these cells during the next two hours, and

was then replaced by new signals in the dorsal epithelium of the trunk, more precisely on and near the midline (Fig. S2.1, EF). At 8 hpf, the expression of *propA* had become more spatially restricted at the axial level of the Nasse cells (Fig. S2.1, G), and it then gradually disappeared through to 12 hpf. The expression of *propB* began shortly after hatching, in eight epithelial cells situated on both sides of the dorsal midline (Fig. S2.1, A'B'C'D'). At 6 hpf, the signal had expanded to neighboring cells and covered a region in and around the midline extending from the Anterior Fol cells to the posterior part of the Anterior rosette (Fig. S2.1, E'F'). At this stage, new signals also appeared in 2–4 cells on the lateral sides of the trunk epithelium that probably border the Fol region. By 8 hpf, the expression of *propB* had slowly decreased in intensity and was observed in cells anterior to the Anterior Fol, on the midline across Giant Fol, Nasse and Posterior Fol

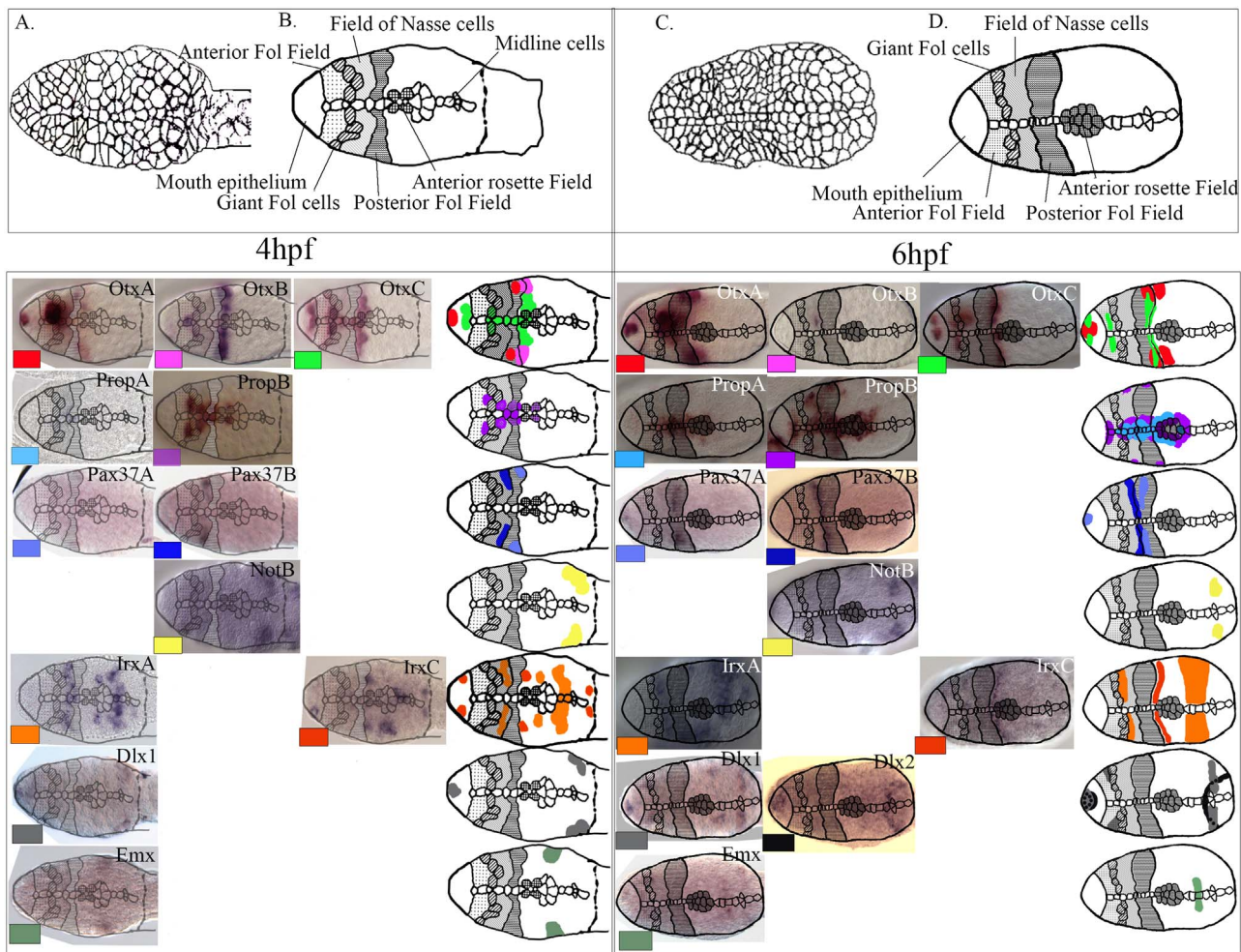


Fig. 2. Schematic representation of homeobox gene expression in the developing epithelium of *Oikopleura dioica*. Presumptive zones of the early larval epithelium at 4 hpf (A,B) and 6 hpf (C,D). The phalloidin staining (A,C) permitted recognition of different cells by shape and size. (B,D) Schematic drawing of the dorsal epithelium based on membrane staining. Overlay of homeobox gene expression patterns with presumptive zones is shown on the schematic drawing of at two time points: 4 and 6 hpf (dorsal view). Larvae are oriented anterior to left. Detailed description of expression patterns is provided in supplementary information.

cells, and in the Anterior rosette (Fig. S2.1, G'). The lateral expression included more expressing cells which formed a line. During later larval development these signals disappeared and we only observed a fuzzy staining where the first pre-house is formed, most likely noise (Fig. S2.1, H'). Double ISH at 6–8 h with *propA* and *propB* gene probes revealed that most cells of the midline expressed either one or the other gene. However, the expression patterns also overlapped in the middle of the Fol region and at the level of the Nasse cells (Fig. 3, A–D). Some co-expression was also observed in Posterior Fol cells and in the posterior spot of the lateral expression domain where the *propB* signal was much stronger.

The genomic organization of *otx* genes is reminiscent of what we found for *prop*-genes. There are three paralogs *otxA*, *otxB* and *otxC* in *O. dioica* and other Oikopleurid species, with at least two of them linked to each other in opposite orientation (the three genes are linked in *O. longicauda*) (Fig. S3.1). Their detailed expression study in *O. dioica* larvae from before hatching until after metamorphosis (Fig. S2.3) showed that all three paralogs were expressed in the cerebral ganglion, possibly reflecting ancestral *otx* function. The CNS expression of *otx* genes during development was also shown previously by C. Cañestro and coauthors, and our images are consistent with theirs (Cañestro and Postlethwait, 2007; Cañestro et al., 2005). All three *otx* genes were also expressed in the developing trunk epithelium. The expression of *otxA* did not overlap those of *otxB* and *otxC*, which were co-expressed in a few lateral epithelial cells at 4–5 hpf. The expression territory of *otxC* was

however much broader. The expression of *otxB* was very high at the earliest stages and was not detectable in the epithelium from 6 hpf onwards. Invertebrates usually have a single *otx* gene, while vertebrates have at least two. We are not aware of any epithelial expression for those. In ascidians however, an intense ISH signal is observed in the developing anterior epidermis at tailbud and larval stages. At least part of it occurs in the precursor region of the adhesive gland (Wada et al., 2004) which does not exist in larvaceans, but we cannot exclude its homology with the most anterior territory expressing *otxA* and *otxC*. This epidermal signal is more anterior than those observed in the developing oikoplastic epithelium proper, found in the Posterior Fol field of *O. dioica* or immediately posterior to it. Overall we propose that the expression of *otx* and *prop* genes in the dorsal epithelium of the larval trunk reflects a lineage-specific co-option for patterning the oikoplastic epithelium. As all five paralogs are expressed there, this co-option probably preceded the gene duplication events.

4. Homeobox gene knockdowns

We initially attempted RNA interference for all three *otx* paralogs. The development of injected embryos was generally abnormal. The amounts of *otxA/B/C* transcripts measured by qPCR were severely reduced but ISH paradoxically showed intense expression signals (Fig. S4). We are therefore unsure whether RNAi successfully induced the knockdown of *otx* genes.

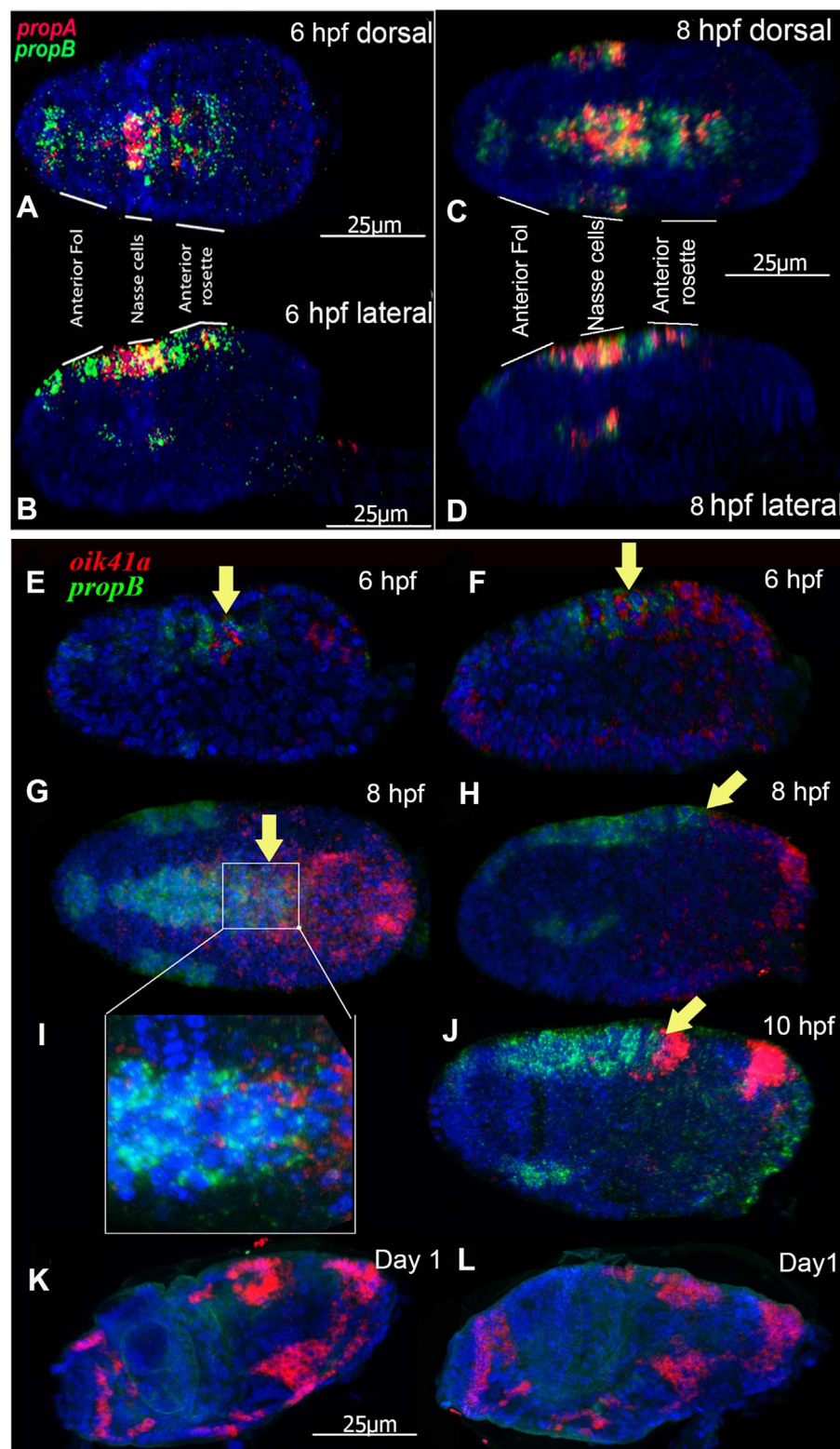
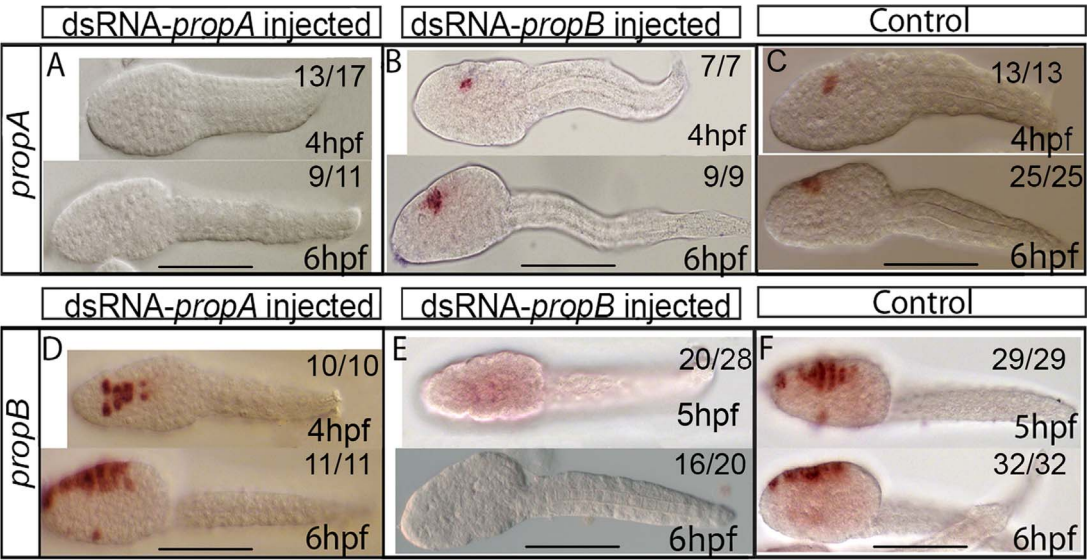


Fig. 3. Spatiotemporal expression patterns of *propA*, *propB* and *oik41a*. **A–D.** Double FISH *propA* (red) and *propB* (green) at 6 hpf (A,B) and 8 hpf (C,D). **A.** *propA* expression was strong in the mid-trunk between the left and right Nasse cell regions. Expression was also detected anterior to the Anterior Fol, and in the anterior part of the prospective Anterior rosette. *propB* was highly expressed along the dorsal epithelial midline, starting anterior to the Anterior Fol, then in the cells situated between the left and right Anterior Fol regions, and more posteriorly, overlapping with expression of *propA* between the Nasse cell regions, and in cells of the prospective Anterior rosette. **E–L.** Co-expression of *propB* (green) and *oik41a* (red) during larval development. **E,** dorsal, and **F,** lateral views of 6 hpf larvae. Expression of *oik41a* occurred in the posterior part of the trunk, and in the region of Anterior rosette, where there was co-expression of *propB*. **G,** dorsal and **H,** lateral views of 8 hpf larvae. Co-expression of *oik41a* and *propB* was visible in the Anterior rosette region. The area of co-expression is magnified (**I**). **J,** lateral view at 10 hpf. Expression of *oik41a* was strong. There was still some co-expression in the region of Anterior rosette. **K,L,** expression of *oik41a* at Day 1. *propB* was not expressed at this stage. *oik41a* mRNA was localized in several epithelial cell types: the mouth ring, lateral cells surrounding the Eisen field, the Posterior rosette, and the Anterior rosette. Arrows indicate zones of co-expression of *propB* and *oik41a*.

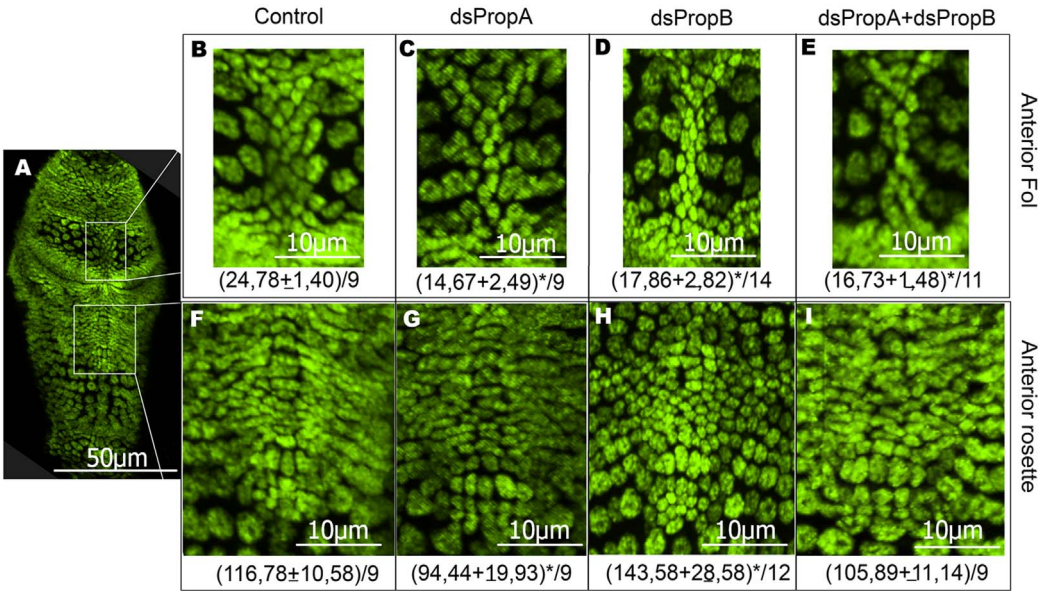
In contrast, RNAi for *prop* genes had marked effects on gene expression, on epithelium development and on the expression of the *oikosin41* gene (Fig. 4). To knock down the expression of *prop* genes, we prepared dsRNA whose sequence matched most of their coding regions (Fig. S3.3). We injected dsRNA-*propA* alone, dsRNA-*propB*

alone or both dsRNA together into unfertilized eggs. Depending on the experiment, 50–80% of the injected eggs divided after fertilization, and some developments stopped after several cell cycles. Embryos that developed normally (20–50% of injected eggs) were collected at 4, 5 and 6 hpf for ISH, and at 5 hpf for RT-qPCR.

1. *in situ* hybridization on dsRNA-injected and control animals



2. Malformation of the epithelium caused by dsRNA-injections.



mRNA level of PropA and PropB after injections of mix dsRNA PropA and dsRNA PropB

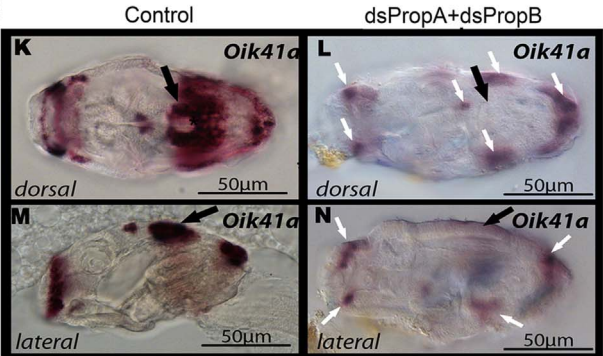
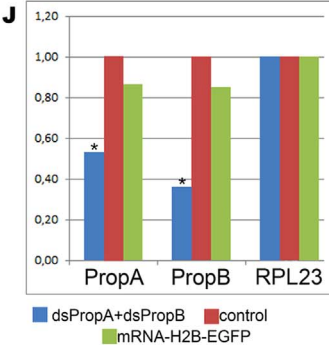


Fig. 4. Alterations of epithelium differentiation after the knockdown of *prop* genes. **1. *in situ* hybridizations.** **A–C:** ISH of *propA* probe at 4–6 hpf on dsRNA-*propA* injected embryos (A), dsRNA-*propB* injected embryos (B) and non-injected embryos (C). Scale: 50 μ m. **D–F:** ISH of *propB* probe on dsRNA-*propA* injected embryos (D), dsRNA-*propB* injected embryos (E) and non-injected embryos (F) at 4–6 hpf. Ratios on pictures (e.g. 13/17) indicate the proportion of animals showing similar expression. **2. Alterations of the epithelium morphology.** **A–I:** Dorsal epithelium at Day1 stained with DAPI (A), with focus on middle cell rows of Anterior Fol (B,C,D,E) and Anterior rosette region (F,G,H,I). Control animals (B,F) show differentiated nuclei with specific shapes and positions. After dsRNA-*propA* injection (C,G), malformations were observed in both regions. After dsRNA-*propB* injection (D,H) nuclei of the midline were rounder, the Anterior rosette was not formed and its nuclei were smaller (H). After dsRNA-*propA*+dsRNA-*propB* injection (E,I), changes were observed in the dorsal midline (E) and the Anterior rosette was not organized (I). The average number of cells were counted in each region for a group of animals (in parentheses; number of animals indicated after /) and significant differences with controls are marked with an asterisk ($p < 0.05$, t -test). **J.** mRNA levels of *propA* or *propB* after dsRNA-*propA*+dsRNA-*propB* injection (blue bars), after injections of control mix with mRNA-EGFP (green bars), in proportion to the values in non-injected controls (red bars). mRNA-RPL23 levels were used as standard to estimate the relative expression levels of *prop* genes ($n > 4$, asterisks indicate significant differences $p < 0.05$, t -test). **K–N.** ISH for *oikodin41a* showed no signal in the Anterior rosette (black arrows) in injected animals (L,N) and intense signal in controls (K,M). White arrows indicate expression of *oikodin41a* outside *prop* gene expression domains.

No ISH signal appeared with the *propA* probe in 77% of dsRNA-*propA* injected larvae (Fig. 4.1A) and the other 23% showed a signal weaker than in controls (Fig. 4.1, C). ISH with the *propB* probe on dsRNA-*propA* injected larvae yielded signals comparable to those of controls (Fig. 4.1, D). The qPCR assays showed a two-fold reduction of *propA* transcript levels. *propB* transcript levels were slightly lower than those in uninjected controls, but comparable to those obtained after injections of a control mix containing EGFP mRNA (Fig. S3.4,A).

ISH with the *propB* gene probe on dsRNA-*propB* larvae showed either no signal (48%) or a markedly reduced signals (23%) or signals comparable to those of controls (29%) (Fig. 4.1, E, F). With the *propA* probe on dsRNA-*propB* animals, the ISH signal in the cerebral ganglion appeared earlier than in controls (Fig. 4.1, BC). It also persisted in the posterior part of the cerebral ganglion until at least 6 hpf (Fig. 4.1, B, 6 hpf) when the ISH signal in controls has already shifted to the dorsal epithelium midline (Fig. 4.1, C 6 hpf; Fig. S2.1, EF). With qPCR, a three-fold reduction of *propB* transcripts was observed following dsRNA-*propB* injection (Fig. S3.4, B).

Injections of dsRNA matching *prop* genes also led to changes in the numbers of nuclei and in the morphology of epithelial territories where they are normally expressed. After injection of dsRNA-*propA*, the number of nuclei was significantly reduced in the Anterior Fol region and in the Anterior rosette (Fig. 4.2, C,G). The shape of nuclei in cells of the of Anterior Fol region middle rows was also changed compared to control animals (Fig. 4.2, C), but their size was not (Fig. 4.2, AE). In the region giving rise to the Anterior rosette, the nuclei became normally elongated, but the Anterior rosette failed to form properly (Fig. 4.2, G). Following dsRNA-*propB* injections, anomalies of midline cells at the level of Anterior Fol were revealed in Day1 animals (Fig. 4.2, D). Their nuclei were round but smaller and more densely packed than normal, and the group of midline cells was overall much narrower than in controls (Fig. 4.2, B). The Anterior rosette (Fig. 4.2, H) was also malformed. There, the number of nuclei was increased. Most of them were rounder and smaller than in control animals, where they reach diverse shapes and sizes (Fig. 4.2, H). The simultaneous knock down of both *prop* genes with both dsRNAs appeared successful, since all ISH signals with either *propA* or *propB* probes virtually disappeared. qPCR showed marked reductions of the transcript levels for both genes, comparable to those observed for each gene after single knockdowns (Fig. 4.2, J). Following dsRNA-*propA*+*propB* injections, the midline essentially consisted of one cell row and nuclei with less sharp contours, versus three cell rows with triangular and compact nuclei in controls (Fig. 4.2, B, E). On each side of this narrower midline, the nuclei are large and round and resemble those of the Anterior Fol field in controls. However, the most striking change after injection of both dsRNAs was a global disorganization of the region where the Anterior rosette is formed (Fig. 4.2, I). There, the midline was hardly distinguishable. Nuclei had poorly defined contours and they did not evolve into the variable shapes (elongated, triangle and square) that they acquired in controls (Fig. 4.2, H).

We finally carried out *in situ* hybridization with an *oikodin41a* gene probe, chosen because it is normally expressed in the Anterior rosette of adults (Hosp et al., 2012). The *oikodin41a* expression patterns and areas of co-expression with *propB* are shown in Fig. 3. Day1 animals were examined for *oikodin41a* expression, in controls and in the

dsRNA-*propA*+*propB* injected group (Fig. 4.2, KLMN). In contrast to observations in Day1 controls, *oikodin41a* was not expressed in the Anterior rosette of injected animals. Several intense ISH signals were detected, after injections and in the controls, in other areas where *prop* genes are not expressed, including the anterior mouth epithelium and the posterior epithelium (Fig. 4.2, LN). Thus, the knockdown of *prop* expression not only impacted the morphology of the Anterior rosette, but also silenced *oikodin41a* expression in this region.

5. Discussion

The oikoplastic epithelium is an exquisitely patterned monolayer of cells that becomes regionalized within a few hours after larval hatching. The territories of the future oikoplastic epithelium appear successively, reach their final number of cells, and the cells and their nuclei adopt characteristic field-specific sizes and shapes. Oikodins in a given territory are expressed either before or after the corresponding territory is fully formed. After metamorphosis, the number of cells remains unchanged and the cells grow through repeated genome endoreduplications. No significant migration of cells is observed between distinct territories. The genetic program underlying the patterning of such a highly specific epithelium is unknown, but relevant candidate players appeared in a systematic ISH expression study of developmental transcription factor genes, first with homeobox genes (Denoeud et al., 2010) and also with Fox genes (Fig. S6). Their ISH signals mark the trunk epithelium during the first half of the larval period and they remain mostly confined to specific areas of the epithelium. The degree to which these signals coincide with specific oikoplastic territories remains to be better assessed, using cell lineage analysis, since the epithelium morphology is not well defined yet when the ISH signals appear. In many cases, both duplicates of one gene are expressed in the epithelium, and their expression domains are similar if not overlapping. For these genes, epithelial expression likely predated the gene duplication events.

The actual involvement of homeobox genes in patterning the oikoplastic epithelium is shown in our functional study of two *prop* genes. They result from a relatively ancient tandem duplication, with orthologs found for both of them in six distinct Oikopleurid species. Interestingly, the duplicates remained next to each other, despite a history of extensive genome rearrangements in the *O. dioica* lineage (Denoeud et al., 2010). Their physical association may have been preserved by functional constraints such as the sharing of common regulatory elements (Irimia et al., 2012; Kikuta et al., 2007). In *O. dioica*, *propA* and *propB* are both expressed in the epithelium of young larvae, on and around the dorsal midline, half way between the anterior and posterior ends of the trunk. Their expression domains are not identical, but they overlapped in several groups of cells. To study their function, we used RNA interference through injection of dsRNA, whose efficiency and specificity were previously validated for five genes, including the notochord master gene *Brachyury*, two genes of neurotransmitter synthesis pathways and two cyclin-dependent kinases (Omotezako et al., 2013; Mikhaleva et al., 2015; Øvrebo et al., 2015). For both *prop* genes, qPCR measurements showed a substantial though incomplete reduction of transcript levels, while the ISH signals generally disappeared. The regions of the epithelium where *prop* genes

are normally expressed were markedly disorganized, with modified cell number, size and/or shape, suggesting interference with cell differentiation processes. We wished to examine whether these cells retained the ability to express specific Oikodin genes which encode proteins of the house. For this, we focused on *oikodin41a*, which is co-expressed together with *prop* genes near the midline of the dorsal epithelium, and is also expressed in more lateral regions of the epithelium where *prop* genes are not expressed (Hosp et al., 2012). After the knockdown of *prop* genes, *oikodin41a* expression remained in these lateral regions, but was no longer expressed around the midline. This observation confirms that *prop* genes are involved, directly or indirectly, in the differentiation of epithelial cells near the dorsal midline, through a field-specific pathway. Before hatching, *propA* was also expressed in the central ganglion, where it possibly exerts an ancestral function (Angotzi et al., 2011; Nakamura et al., 1999; Sornson et al., 1996). This expression was efficiently knocked down without compromising survival until after metamorphosis. The three *otx* genes show high levels of regionalized expression in the epithelium. The same three paralogs are all found in all Oikopleurid species that we surveyed and they also show physical linkages. In addition to the epithelium, they are also expressed in the CNS. In larvae that survived after dsRNA injections, strong gene-specific ISH signals were maintained. Either the knockdown did not happen, or embryos died at an early stage when it occurred. We were therefore unable to demonstrate the involvement of *otx* genes in the fate of epithelial cells.

Most homeobox genes expressed in the trunk epithelium are duplicated. One notable exception is *hox2*, exclusively expressed in ventral epithelial cells with a characteristic pattern (one transversal row and two lateral dots). This gene probably lost its ancestral function (Seo et al., 2004), since all other Hox genes are expressed in the tail, with *hox1* expressed anteriorly near the tail-trunk junction and *hox13* expressed posteriorly near the tail tip. Thus far, the most parsimonious scenario for the history of Oikopleura homeobox genes can be summarized as follows. A relatively large proportion of ancestral genes were lost, and the others conserved their original function or were recruited for patterning the oikoplastic epithelium. Those that did so are often duplicated and their copies conserved this new expression, which could be either broadened through neofunctionalization or became more specialized through subfunctionalization. Depending on the genes, the ancestral function(s) may have been lost prior to or after the duplication events. Overall, the major novelty that the house represents may have favored the retention of homeobox gene groups, in a more general context of frequent gene loss, which may be related to a morphological simplification of tunicates and/or larvaceans. Duplications were probably not required for the emergence of the oikoplastic epithelium. However, it is possible that they played a role to increase the complexity of its patterning.

6. Materials and methods

6.1. Animal collection

Populations maintained in culture originated from fjords near Bergen, Norway. The life cycle in culture lasts for 6 days at 13–14 °C (Bouquet et al., 2009). Sexually mature adults were transferred at Day 6 into separate containers: 5 males into a container with 10 ml of filtrated artificial seawater (FASW) (final salinity 30.2 g/l, Red Sea Europe, ZA de la St-Denis, France); each female into its individual container (Cat. no. 631–9301, VWR, Oslo, Norway) with 5 ml of FASW. Females were washed several times with artificial seawater to prevent uncontrolled fertilization. Spawned oocytes were fertilized with 50 µl of sperm solution and developed to the embryonic or larval stage of interest at 16–17 °C. Development to Day1 (beyond metamorphosis) occurred overnight in 10 ml plastic tubes filled with FASW placed on a rotating wheel. Later development occurred in 6-liter beakers, from which juveniles were collected at various stages and transferred into

watch glasses for gentle removal of their house. Addition of the anesthetic MS222 (0.25 mg/ml; Sigma, St. Louis, MO, USA) in the FASW prevented the production of new houses before fixation. The medium with anesthetic was replaced by fixative (4% PAF) that was renewed once. Fixation lasts for one hour at room temperature or 1–2 days at 4 °C.

6.2. Epithelium development and confocal microscopy

Animals were fixed as for the ISH protocol, and the nuclei were stained with either TOPRO-3 (red) (Thermo Fisher Scientific, Waltham, MA USA) or SYBR-green (Molecular Probes, Eugene, OR USA). At least three animals were observed for each stage. The confocal microscope was set to optically section the animal trunk at 0.55 µm intervals.

6.3. Synthesis of RNA probes for ISH

PCR primers used for probe synthesis are given in Table S 1. PCR products from each gene were cloned into pGemT-easy vector (A1360, Promega, Oslo, Norway) and sequenced before *in vitro* transcription. Probes were labeled with DIG-labeling mix (Roche, Oslo, Norway) for *propA*, *propB*, Oikodin genes and Fluorescein labeling mix (Roche, Oslo, Norway) for *propB*.

6.4. Whole mount in situ hybridization and fluorescent in situ hybridization

The ISH protocol was described in Mikhaleva et al. (2015). Double fluorescence ISH was performed as follows: both probes with different labeling at a concentration of 1 ng/µl were simultaneously added into hybridization buffer for overnight incubation at 60 °C. Washing steps and RNase treatment were carried out as for non-fluorescence *in situ* hybridization. Animals were then washed in RNase buffer (30 min, 60 °C), twice in PBT (2 × 5 min at room temperature), in 3% H₂O₂/PBT (30 min at room temperature) and finally twice with PBT (5 min at room temperature each time). Blocking (1% blocking reagent solution (cat. no. 11096176001, Roche, Oslo, Norway) in PBS, 0.1% Triton- X) was performed for at least one hour at room temperature with continuous shaking. Anti-fluorescein antibody conjugated with POD (1:1000 in blocking solution) (Roche, Oslo, Norway) was added to samples for overnight incubation at 4 °C. The day after, samples were washed three times with PBT for 15 min at room temperature, once with dilution buffer of TSA kit and then stained for one hour with TSA-fluorescein (Perkin-Elmer, Boston, MA) at 1/50 dilution. They were then washed three times with PBT (5 min at room temperature), once with 3% H₂O₂/PBT (30 min at room temperature), once with PBT (5 min at room temperature) before blocking was carried out for at least one hour at room temperature (as described above). Anti-dioxigenin antibody conjugated with POD (1:300 in blocking solution) was added to samples for overnight incubation at 4 °C. The morning after, samples were washed three times with PBT (15 min at room temperature), once with dilution buffer of TSA kit and then stained for two hours with TSA-Cy5 (Perkin-Elmer, Boston, MA) at 1/50 dilution. After staining embryos were washed three times with PBT (15 min at room temperature). Mounting was done in SlowFade® Gold antifade reagent with DAPI (S36938, Molecular Probes, OR). For detection of early Oikodin transcripts, ISH was optimized: 0.1% Tween and 1 mM EDTA were added to all solutions beginning with fixation and until the last washing step. The only solution that was used without adding 0.1% Tween/1 mM EDTA was the TSA diluent. A Nikon Eclipse E800 compound microscope was used for imaging of samples using the 40x objective. Pictures were taken with a Nikon Digital Sight DSU3 camera. Fluorescent signals were observed with a Leica SP5 confocal microscope. Imaris software (Bitplane AG) was used for 3D reconstruction of confocal series. Figures were composed using Adobe Photoshop CS5. Images were cropped and adjusted for brightness/contrast. Any such adjustment was applied to the entire image.

6.5. RNA interference

PCR products obtained with the primers listed below were cloned into the L4440 vector, sequenced and used for transformation of HT115 E.coli strain (Asencio et al., 2003) for dsRNA production. Primer sequences for preparation of dsRNA are given in Table S1. dsRNA purification from bacteria was performed as described (Mikhaleva et al., 2015). After dsRNA purification with TRIzol (cat.no. 15596–026, Life Technologies, Oslo, Norway), acid phenol/chloroform extraction and alcohol precipitation were performed to remove residual bacterial proteins. Concentrations of dsRNA were estimated using a nanodrop ND-1000 spectrophotometer. The final concentration of dsRNA in the injection mix (ddH₂O, Dextran Alexa568 in final concentration 65 mg/ml (cat.no. D22912, Life Technologies), was 500 ng/μl for *propA* and *propB*. Preparations of injection needles, oocyte holding pipettes, filtered artificial sea water and sperm solution were described previously (Mikhaleva et al., 2015). The dsRNA mix, or control mix without dsRNA (ddH₂O, Dextran Alexa568 in final concentration 65 mg/ml, were injected into unfertilized oocytes. Oocytes were repeatedly washed with 25 mM Ca²⁺ in FASW for two minutes, incubated for 10–15 min, and then transferred onto a plate for microinjections, where they were divided into control and injected groups. Control oocytes and injected oocytes from one female were transferred into 6-well tissue plates (cat.no. 392–0036, VWR, Oslo, Norway) covered with 1% agarose (cat. no. V3121, Promega, Oslo, Norway). The injection procedure was repeated for several females during 2–3 h. Injected oocytes from each female were placed into separate wells. *In vitro* fertilization was performed with 50 μl of sperm solution simultaneously for all oocytes from an injection session. Development was stopped either by fixation in 4% PAF for ISH or by freezing in liquid nitrogen for RNA isolation.

6.6. RT-qPCR

Total RNA was isolated from 50 to 75 animals (5hpf) with RNAqueous®-Micro Total RNA Isolation Kit (AM 1931, Ambion, Oslo, Norway) and DNase treated with reagents included into the kit according to manufacturer instructions. Total RNA concentration was estimated on an aliquot with Agilent 2100 Bioanalyzer system (Agilent Technologies, USA). An equal amount of total RNA was used to generate ssDNA (SuperScriptIII reverse transcriptase kit (Invitrogen, 18080-098) with oligo(dT) primers). RT-qPCR was performed using iQ SYBR Green Supermix (Bio-Rad, 170–8880). Several primer pairs were tested to maximize efficiency (at least 99%) and obtain a single peak of the melting curve. RT-qPCR was performed with BioRAD-qPCR Detection System using the following cycle: denaturation at 95 °C for 3 min, 39 cycles at 95 °C for 10 s, 60 °C for 30 s and 72 °C for 30 s, with final extension at 55 °C for 30 s, with following increase of temperature from 0.5 °C to 95 °C. The levels of *propA/propB* mRNA expression after dsRNA injection and control mix injection were normalized against RPL23 (ribosomal protein 23) gene expression. Relative changes of mRNA levels between injected and control animals were calculated using the comparative method of relative quantification (Pfaffl, 2001). Primers used for RT-qPCR analysis are given in Table S1.

Acknowledgements

We would like to thank Jean-Marie Bouquet and the staff of Appy Park for their efforts in culturing *Oikopleura*. We also thank the personnel of Genoscope (Evry, France), Marit Flo Jensen, Hee-Chan Seo and Rolf B. Edvardsen for their early contribution in *Oikopleura* gene annotation and studies of expression patterns.

Competing interests

No competing interests declared.

Author contributions

Author contributions E.T. and R.S. performed studies of early Oikotin gene expression and larval epithelium development, Y.M. performed the RNAi experiments and filming the epithelium development, and D.C. performed all gene annotations and phylogenetic analysis and supervised the homeobox gene project. S.S. assembled the genomes of all larvacean species others than *Oikopleura dioica*. All authors contributed to the preparation of the manuscript.

Funding

This project has been funded by three major grants of the Research Council of Norway of which Daniel Chourrout is the PI: ES424062 OIKOSYS, 250005 accelerated evolution in chordates and the origin of larvaceans, 234817 Sars International Centre for Marine Molecular Biology Research, 2013–2022.

Summary statement

The house, a spectacular innovation of tunicate larvaceans used for filter feeding, is synthesized by a complex epithelium, whose formation is shown to involve multiple homeodomain transcription factors.

Appendix A. Supporting information

Supplementary data associated with this article can be found in the online version at doi:10.1016/j.ydbio.2018.09.006.

References

- Andersson, D.I., Jerlström-Hultqvist, J., Näsvall, J., 2015. Evolution of new functions de novo and from preexisting genes. *Cold Spring Harb. Perspect. Biol.* 7, a017996.
- Angotzi, A.R., Mungpakdee, S., Stefansson, S., Male, R., Chourrout, D., 2011. General and comparative endocrinology involvement of Prop1 homeobox gene in the early development of fish pituitary gland. *Gen. Comp. Endocrinol.* 171, 332–340.
- Asencio, C., Rodriguez-Aguilera, J.C., Ruiz-Ferrer, M., Vela, J., Navas, P., 2003. Silencing of ubiquitinone biosynthesis genes extends life span in *Caenorhabditis elegans*. *FASEB J.* 17, 1135–1137.
- Bouquet, J.M., Spriet, E., Troedsson, C., Ottera, H., Chourrout, D., Thompson, E.M., 2009. Culture optimization for the emergent zooplanktonic model organism *Oikopleura dioica*. *J. Plankt. Res.* 31, 359–370.
- Cañestro, C., Postlethwait, J.H., 2007. Development of a chordate anterior-posterior axis without classical retinoic acid signaling. *Dev. Biol.* 305, 522–538.
- Cañestro, C., Bassham, S., Postlethwait, J., 2005. Development of the central nervous system in the larvacean *Oikopleura dioica* and the evolution of the chordate brain. *Dev. Biol.* 285, 298–315.
- Carroll, S.B., 2008. Evo-Devo and an expanding evolutionary synthesis: a genetic theory of morphological evolution. *Cell* 134, 25–36.
- De Robertis, E.M., 2008. Evo-devo: variations on ancestral themes. *Cell* 132, 185–195.
- Delsuc, F., Brinkmann, H., Chourrout, D., Philippe, H., 2006. Tunicates and not cephalochordates are the closest living relatives of vertebrates. *Nature* 439, 965–968.
- Denoeud, F., Henriot, S., Mungpakdee, S., Aury, J.-M., Da Silva, C., Brinkmann, H., Mikhaleva, Y., Olsen, L.C., Jubin, C., Cañestro, C., et al., 2010. Plasticity of animal genome architecture unmasked by rapid evolution of a pelagic tunicate. *Science* (80-.) 330, 1381–1385.
- Dittmar, K., Liberles, D.A., 2010. Evolution After Gene Duplication 2011. John Wiley & Sons, Hoboken, NJ, USA.
- Duboule, D., 2010. The evo-devo comet. *EMBO Rep.* 11, 489.
- Edvardsen, R.B., Seo, H.-C., Jensen, M.F., Mialon, A., Mikhaleva, J., Bjordal, M., Cartry, J., Reinhardt, R., Weissenbach, J., Wincker, P., et al., 2005. Remodelling of the homeobox gene complement in the tunicate *Oikopleura dioica*. *Curr. Biol.* 15, R12–R13.
- Galant, R., Carroll, S.B., 2002. Evolution of a transcriptional repression domain in an insect Hox protein. *Nature* 415, 910–913.
- Ganot, P., Thompson, E.M., 2002. Patterning through differential endoreduplication in epithelial organogenesis of the Chordate, *Oikopleura dioica*. *Dev. Biol.* 252, 59–71.
- Hosp, J., Sagane, Y., Danks, G., Thompson, E.M., 2012. The evolving proteome of a complex extracellular matrix, the *Oikopleura* house. *PLoS One* 7, e40172.
- Huminecki, L., Wolfe, K.H., 2004. Divergence of spatial gene expression profiles following species-specific gene duplications in human and mouse. *Genome Res.* 14,

- 1870–1879.
- Imai, K.S., Hino, K., Yagi, K., Satoh, N., Satou, Y., 2004. Gene expression profiles of transcription factors and signaling molecules in the ascidian embryo: towards a comprehensive understanding of gene networks. *Development* 131, 4047–4058.
- Irimia, M., Royo, J.L., Burguera, D., Maeso, I., Gómez-Skarmeta, J.L., Garcia-Fernandez, J., 2012. Comparative genomics of the Hedgehog loci in chordates and the origins of Shh regulatory novelties. *Sci. Rep.* 2, 1–9.
- Kikuta, H., Laplante, M., Navratilova, P., Komisarczuk, A.Z., Engstrom, P.G., Fredman, D., Akalin, A., Caccamo, M., Sealy, I., Howe, K., et al., 2007. Genomic regulatory blocks encompass multiple neighboring genes and maintain conserved synteny in vertebrates. *Genome Res.* 17, 545–555.
- Kishi, K., Hayashi, M., Onuma, T.A., Nishida, H., 2017. Patterning and morphogenesis of the intricate but stereotyped oikoplastic epidermis of the appendicularian, *Oikopleura dioica*. *Dev. Biol.* 428, 245–257.
- Koshikawa, S., Giorgianni, M.W., Vaccaro, K., Kassner, V. a., Yoder, J.H., Werner, T., Carroll, S.B., 2015. Gain of cis-regulatory activities underlies novel domains of wingless gene expression in *Drosophila*. *Proc. Natl. Acad. Sci. USA* 112, 7524–7529.
- Lynch, V.J., Wagner, G.P., 2008. Resurrecting the role of transcription factor change in developmental evolution. *Evolution* 62, 2131–2154.
- Mikhaleva, Y., Kreneisz, O., Olsen, L.C., Glover, J.C., Chourrout, D., 2015. Modification of the larval swimming behavior in *Oikopleura dioica*, a chordate with a miniaturized central nervous system by dsRNA injection into fertilized eggs. *J. Exp. Zool. B. Mol. Dev. Evol.* 324, 114–127.
- Ming, R., VanBuren, R., Wai, C.M., Tang, H., Schatz, M.C., Bowers, J.E., Lyons, E., Wang, M.-L., Chen, J., Biggers, E., et al., 2015. The pineapple genome and the evolution of CAM photosynthesis. *Nat. Genet.* 47, 1435–1442.
- Moriyama, Y., Ito, F., Takeda, H., Yano, T., Okabe, M., Kuraku, S., Keeley, F.W., Koshiba-Takeuchi, K., 2016. Evolution of the fish heart by sub/neofunctionalization of an elastin gene. *Nat. Commun.* 7, 10397.
- Nakamura, Y., Usui, T., Mizuta, H., Murabe, H., Muro, S., Suda, M., Nakao, K., 1999. Characterization of Prophet of Pit-1 gene expression in normal pituitary and pituitary adenomas in humans. *J. Clinical Endocrinol. Metabolism* 84 (4), 1414–1419.
- Ohno S. (1970). Evolution by gene duplication.**
- Omotezako, T., Nishino, A., Onuma, T. a., Nishida, H., 2013. RNA interference in the appendicularian *Oikopleura dioica* reveals the function of the Brachyury gene. *Dev. Genes Evol.* 223, 261–267.
- Øvrebo, J.I., Campsteijn, C., Kourtesis, I., Hausen, H., Raasholm, M., Thompson, E.M., 2015. Functional specialization of chordate CDK1 paralogs during oogenic meiosis. *Cell Cycle* 14 (6), 880–893.
- Pfaffl, M.W., 2001. A new mathematical model for relative quantification in real-time RT-PCR. *Nucleic Acids Res.* 29, e45.
- Sagane, Y., Zech, K., Bouquet, J.M., et al., 2010. Functional specialization of cellulose synthase genes of prokaryotic origin in chordate larvaceans. *Development* 137, 1483–1492.
- Sagane, Y., Hosp, J., Zech, K., Thompson, E.M., 2011. Cytoskeleton-mediated templating of complex cellulose-scaffolded extracellular structure and its association with oikosins in the urochordate *Oikopleura*. *Cell. Mol. Life Sci.* 68, 1611–1622.
- Seo, H., Edvardsen, R.B., Maeland, A.D., Bjordal, M., Jensen, M.F., Hansen, A., Flaas, M., Weissenbach, J., Lehrach, H., Wincker, P., et al., 2004. Hox cluster disintegration with persistent anteroposterior order of expression in *Oikopleura dioica*. *Nature* 431, 67–71.
- Sornson, M.W., Wu, W., Dasen, J.S., Flynn, S.E., Norman, D.J., O'Connell, S.M., Gukovsky, I., Carrière, C., Ryan, a.K., Miller, a.P., et al., 1996. Pituitary lineage determination by the Prophet of Pit-1 homeodomain factor defective in Ames dwarfism. *Nature* 384, 327–333.
- Spada, F., Steen, H., Troedsson, C., Kallesoe, T., Spriet, E., Mann, M., Thompson, E.M., 2001. Molecular patterning of the oikoplastic epithelium of the larvacean tunicate *Oikopleura dioica*. *J. Biol. Chem.* 276, 20624–20632.
- Tautz, D., Domazet-Lošo, T., 2011. The evolutionary origin of orphan genes. *Nat. Rev. Genet.* 12, 692–702.
- Wada, S., Tokuoka, M., Shoguchi, E., Spagnuolo, A., Branno, M., Kohara, Y., Rokhsar, D., Levine, M., Saiga, H., Satoh, N., et al., 2003. A genomewide survey of developmentally relevant genes in *Ciona intestinalis*. II. Genes for homeobox transcription factors. *Dev. Genes Evol.* A genomewide survey of developmentally relevant genes in *Ciona intestinalis* II. Genes for homeobox transcription. *Dev. Genes Evol.* 213, 222–234.
- Wada, S., Sudou, N., Saiga, H., 2004. Roles of Hroth, the ascidian otx gene, in the differentiation of the brain (sensory vesicle) and anterior trunk epidermis in the larval development of *Halocynthia roretzi*. *Mech. Dev.* 121, 463–474.
- Wallace, A., 2002. The emerging conceptual framework of evolutionary developmental biology. *Nature* 415, 757–764.
- Wray, K.B., 2007. The age-old question of researcher innovation. *Science* 318, 1549–1550.